

# Intermittent operation of QC-lasers for mid-IR spectroscopy with low heat dissipation: tuning characteristics and driving electronics

M. Fischer,<sup>1</sup> B. Tuzson,<sup>1,\*</sup> A. Hugi,<sup>1,4</sup> R. Brönnimann,<sup>2</sup> A. Kunz,<sup>2</sup>  
S. Blaser,<sup>3</sup> M. Rochat,<sup>3</sup> O. Landry,<sup>3</sup> A. Müller,<sup>3</sup> and L. Emmenegger<sup>1</sup>

<sup>1</sup>*Empa, Laboratory for Air Pollution and Environmental Technology,  
Überlandstr. 129, 8600 Dübendorf, Switzerland*

<sup>2</sup>*Empa, Laboratory for Electronics, Metrology and Reliability,  
Überlandstr. 129, 8600 Dübendorf, Switzerland*

<sup>3</sup>*Alpes Lasers SA, 1-3 Maximilien-de-Meuron, 2001 Neuchâtel, Switzerland*

<sup>4</sup>*ETH Zurich, Institute for Quantum Electronics, 8093 Zurich, Switzerland*

[\\*bela.tuzson@empa.ch](mailto:bela.tuzson@empa.ch)

**Abstract:** Intermittent scanning for continuous-wave quantum cascade lasers is proposed along with a custom-built laser driver optimized for such operation. This approach lowers the overall heat dissipation of the laser by dropping its drive current to zero between individual scans and holding a longer pause between scans. This allows packaging cw-QCLs in TO-3 housings with built-in collimating optics, thus reducing cost and footprint of the device. The fully integrated, largely analog, yet flexible laser driver eliminates the need for any external electronics for current modulation, lowers the demands on power supply performance, and allows shaping of the tuning current in a wide range. Optimized ramp shape selection leads to large and nearly linear frequency tuning ( $> 1.5 \text{ cm}^{-1}$ ). Experimental characterization of the proposed scheme with a QCL emitting at  $7.7 \mu\text{m}$  gave a frequency stability of  $3.2 \times 10^{-5} \text{ cm}^{-1}$  for the laser emission, while a temperature dependence of  $2.3 \times 10^{-4} \text{ cm}^{-1}/\text{K}$  was observed when the driver electronics was exposed to sudden temperature changes. We show that these characteristics make the driver suitable for high precision trace gas measurements by analyzing methane absorption lines in the respective spectral region.

© 2014 Optical Society of America

**OCIS codes:** (140.5965) Semiconductor lasers, quantum cascade; (300.6340) Spectroscopy, infrared; (300.6360) Spectroscopy, laser.

## References and links

1. F. Tittel, Y. A. Bakhrkin, R. Curl, A. Kosterev, M. McCurdy, S. So, and G. Wysocki, "Laser based chemical sensor technology: Recent advances and applications" in *Advanced Environmental Monitoring*, Y. Kim and U. Platt, eds. (Springer Netherlands, 2008), pp. 50–63.
2. R. Curl, F. Capasso, C. Gmachl, A. Kosterev, B. McManus, R. Lewicki, M. Pusharsky, G. Wysocki, and F. Tittel, "Quantum cascade lasers in chemical physics," *Chem. Phys. Lett.* **487**, 1–18 (2010).
3. B. Tuzson, M. Mangold, H. Looser, A. Manninen, and L. Emmenegger, "Compact multipass optical cell for laser spectroscopy," *Opt. Lett.* **38**, 257–259 (2013).

4. Y. Yao, A. J. Hoffman, and C. F. Gmachl, "Mid-infrared quantum cascade lasers," *Nat. Photon.* **6**, 432–439 (2012).
5. M. Taubman, "Note: Switch-mode hybrid current controllers for quantum cascade lasers," *Rev. Sci. Instrum.* **84**, 016103 (2013).
6. S. Blaser, A. Bachle, S. Jochum, L. Hvozdar, G. Vandeputte, S. Brunner, S. Hansmann, A. Muller, and J. Faist, "Low-consumption (below 2 W) continuous wave single mode quantum-cascade lasers grown by metal-organic vapour-phase epitaxy," *Electron. Lett.* **43**, 1201–1202 (2007).
7. Y. Bai, S. R. Darvish, N. Bandyopadhyay, S. Slivken, and M. Razeghi, "Optimizing facet coating of quantum cascade lasers for low power consumption," *J. Appl. Phys.* **109**, 053103, (2011).
8. B. Hinkov, A. Bismuto, Y. Bonetti, M. Beck, S. Blaser, and J. Faist, "Single-mode quantum cascade lasers with power dissipation below 1 W," *Electron. Lett.* **48**, 646–647 (2012).
9. L. Tombez, F. Cappelli, S. Schilt, G. Di Domenico, S. Bartalini, and D. Hofstetter, "Wavelength tuning and thermal dynamics of continuous-wave mid-infrared distributed feedback quantum cascade lasers," *Appl. Phys. Lett.* **103**, 031111 (2013).
10. K. Namjou, S. Cai, E. A. Whittaker, J. Faist, C. Gmachl, F. Capasso, D. Sivco, and A. Cho, "Sensitive absorption spectroscopy with a room-temperature distributed-feedback quantum-cascade laser," *Opt. Lett.* **23**, 219–221 (1998).
11. E. Normand, M. McCulloch, G. Duxbury, and N. Langford, "Fast, real-time spectrometer based on a pulsed quantum-cascade laser," *Opt. Lett.* **28**, 16–18 (2003).
12. D. Nelson, J. Shorter, J. McManus, and M. Zahniser, "Sub-part-per-billion detection of nitric oxide in air using a thermoelectrically cooled mid-infrared quantum cascade laser spectrometer," *Appl. Phys. B* **75**, 343–350 (2002).
13. J. McManus, D. Nelson, S. Herndon, J. Shorter, M. Zahniser, S. Blaser, L. Hvozdar, A. Muller, M. Giovannini, and J. Faist, "Comparison of cw and pulsed operation with a TE-cooled quantum cascade infrared laser for detection of nitric oxide at  $1900\text{ cm}^{-1}$ ," *Appl. Phys. B* **85**, 235–241 (2006).
14. M. McCulloch, E. Normand, N. Langford, G. Duxbury, and D. Newnham, "Highly sensitive detection of trace gases using the time-resolved frequency downchirp from pulsed quantum-cascade lasers," *J. Opt. Soc. Am. B* **20**, 1761–1768 (2003).
15. A. Kosterev, R. Curl, F. Tittel, C. Gmachl, F. Capasso, D. Sivco, J. Baillargeon, A. Hutchinson, and A. Cho, "Effective utilization of quantum-cascade distributed-feedback lasers in absorption spectroscopy," *Appl. Opt.* **39**, 4425–4430 (2000).
16. J. Faist, *Quantum Cascade Lasers*, (Oxford University, 2013).
17. H. Li, "Refractive index of silicon and germanium and its wavelength and temperature derivatives," *J. Phys. Chem. Ref. Data* **9**, 562–658 (1980).
18. P. Werle, R. Mücke, and F. Slemr, "The limits of signal averaging in atmospheric trace-gas monitoring by tunable diode-laser absorption spectroscopy (TDLAS)," *Appl. Phys. B* **57**, 131–139 (1993).
19. L. Tombez, J. Di Francesco, S. Schilt, G. Di Domenico, J. Faist, P. Thomann, and D. Hofstetter, "Frequency noise of free-running  $4.6\text{ }\mu\text{m}$  distributed feedback quantum cascade lasers near room temperature," *Opt. Lett.* **36**, 3109–3111 (2011).
20. L. Rothman, I. Gordon, A. Barbe, D. Benner, P. Bernath, M. Birk, V. Boudon, L. Brown, A. Campargue, J.-P. Champion, K. Chance, L. Coudert, V. Dana, V. Devi, S. Fally, J.-M. Flaud, R. Gamache, A. Goldman, D. Jacquemart, I. Kleiner, N. Lacome, W. Lafferty, J.-Y. Mandin, S. Massie, S. Mikhailenko, C. Miller, N. Moazzen-Ahmadi, O. Naumenko, A. Nikitin, J. Orphal, V. Perevalov, A. Perrin, A. Predoi-Cross, C. Rinsland, M. Rotger, M. M. Šimečková, M. Smith, K. Sung, S. Tashkun, J. Tennyson, R. Toth, A. Vandaele, and J. V. Auwera, "The HITRAN 2008 molecular spectroscopic database," *J. Quant. Spectrosc. Ra.* **110**, 533–572 (2009).
21. P. Varghese and R. Hanson, "Collisional narrowing effects on spectral line shapes measured at high resolution," *Appl. Opt.* **23**, 2376–2385 (1984).
22. B. Tuzson, K. Zeyer, M. Steinbacher, J. B. McManus, D. D. Nelson, M. S. Zahniser, and L. Emmenegger, "Selective measurements of NO, NO<sub>2</sub> and NO<sub>y</sub> in the free troposphere using quantum cascade laser spectroscopy," *Atmos. Meas. Techn.* **6**, 927–936 (2013).
23. G. W. Santoni, B. H. Lee, J. P. Goodrich, R. K. Varner, P. M. Crill, J. B. McManus, D. D. Nelson, M. S. Zahniser, and S. C. Wofsy, "Mass fluxes and isofluxes of methane (CH<sub>4</sub>) at a New Hampshire fen measured by a continuous wave quantum cascade laser spectrometer," *J. Geophys. Res.* **D 117** (2012).

## 1. Introduction

Recent advances in mid-infrared (MIR) laser technology have triggered an impressive progress in instrumental developments. These analytical tools are increasingly employed in a broad area of applications ranging from environmental science to industrial process control as well as medical diagnostics [1, and references therein]. With the advent of room-temperature, high power, and continuous-wave (cw) quantum cascade (QC) distributed feedback (DFB) lasers a large

variety of measurement techniques have been proposed, successfully demonstrated and even brought to commercial products (see review by [2, and references therein]). Despite the many different detection schemes, there is one common property that emerges: the ultimate quest for compact, easy-to-use, reliable, and low-cost optical analyzers for high precision, multi-species measurements. The high output power of cw-QCLs allows using thermoelectrically cooled (TEC) small footprint IR-detectors which, combined with novel absorption cells, is an important step towards ultra-compact optical designs [22]. However, there are still major obstacles in further reducing the overall instrumental size. At present, most of the QCL devices require high current (several hundred of mA) for their cw-operation and thus have high power dissipation [4]. Thus, driver development for this type of lasers is highly demanding with respect to temperature stability and noise level [5]. Furthermore, the significant heat dissipation of the QCLs requires bulky heat-management and temperature control systems, especially for low operating temperatures. In addition to these issues, the beam emitted by QCLs, similar to other semiconductor laser, inherently exhibits a large divergence angle (up to  $60^\circ$ ) due to the strong diffraction at the chip facet caused by the tightly confined waveguide. Thus, an additional collimating element is needed to shape and couple the laser beam into the rest of the optical system. Currently, instrument manufacturers are mainly relying on three different packages for QC laser sources: the benchtop laboratory laser housing (LLH) with a volume of  $174\text{ cm}^3$ , the high heat load (HHL) housing ( $20\text{ cm}^3$ ), and TO-3 cans ( $5\text{ cm}^3$ ) with pulsed QCL. Considering size, cost and complexity, the TO-3 packaging, preferentially with integrated fast optics for collimation, would clearly be the industry's choice if they were available also with cw-QCL. However, the heat dissipation capacity of TO-3 packages with integrated Peltier element is only  $<0.5\text{ W}$  when the laser chip needs to be cooled by  $25^\circ\text{C}$  compared to 8 and 22 W for the HHL and LLH, respectively. Therefore, most of the QCLs cannot be mounted into such housings and alternative approaches are required. There are ongoing developments in the design of lasers and the optimization of the fabrication processes and QCLs with threshold power dissipation down to 1 W were demonstrated [6, 7, 8]. Regardless of the wall-plug efficiency of the deployed laser, the intermittent driving of cw-QCLs proposed in this work allows to considerably ( $<90\%$ ) reduce the power dissipation of the devices, opening the way to very compact and portable sensors based on QCLs.

Generally, for trace gas absorption measurements, the cw emission frequency of a DFB QCL is repeatedly scanned over a molecular absorption profile upon the thermal tuning of the refractive index of the waveguide. A fast and periodic change in the temperature of the DFB laser's active region is achieved via resistive Joule heating by using an externally modulated DC power supply, capable of delivering high currents (up to 1 A). The small cross section of the QCLs active region allows temperature modulation on the order of several hundreds of kHz, mainly limited by the thermal dynamics of the device [9]. However, such modulation scheme would require high-speed detection and data acquisition electronics. Therefore, the rate of the current sweep is typically in the order of few kHz that can be realized by relatively slow and cost-effective devices.

Pulsed operation schemes have extensively been investigated, especially before the development of cw-QCLs. They feature reduced average power consumption compared to the cw-operation, but at the cost of lower signal-to-noise ratio (SNR), broader line width and generally more complex driving electronics. Two major concepts were proposed: the inter-pulse [10] and intra-pulse [11] strategy. For inter-pulse operation, usually short (5 - 10 ns) current pulses are used with a repetition rate of up to MHz. A few kHz sub-threshold current ramp is superimposed to the excitation pulse train for laser frequency tuning and thus an absorption spectrum is built-up from a few hundred to thousands points, corresponding to individual current pulses [12]. Nevertheless, pulsed operation puts stringent requirements on the detectors (speed and

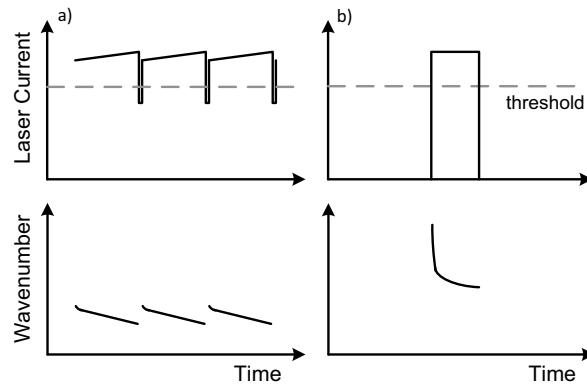


Fig. 1. Laser modulation schemes: a) Standard modulation used for spectroscopy. A saw tooth waveform modulates the laser current in a narrow range around a fixed set-point above the threshold (top). For a sufficiently slow modulation the emission wavelength follows the current (bottom). b) Intermittent modulation with reduced duty cycle. The enhanced temperature chirp at the beginning of the scan causes a large tuning and the emission frequency is slightly blue shifted, even though the temperature of the laser heat sink is the same.

sensitivity) and pulse-to-pulse variations can seriously limit the achievable SNR by introducing amplitude noise. In addition, the rapid changes of current that occur with such a short pulse excitation inherently lead to strong frequency chirping and to significant increase in laser line width ( $\sim 400$  MHz), reducing the spectral resolution of the analyzer [13]. In the case of intra-pulse measurements, the laser is typically driven by current pulses with 200 ns to 1  $\mu$ s duration and relies on the linear frequency down-chirp effect. This method allows to acquire the full spectral information during a single laser pulse without any additional sub-threshold current ramp modulation. Also a wider tuning range is accessible with a more linear function of the scan time. Although, the resolution limitations of both the inter-pulse and the intra-pulse methods are set by the transform limit of the pulse or the bandwidth-time-duration product of the signal detected by the detection system [14], the latter approach avoids the limitations associated to increased effective line width, but has a severe requirement on the bandwidth ( $\sim 1$  GHz) of the detection system.

An alternative approach, which combines the advantage of pulsed and cw-operations, was proposed by [15] for liquid nitrogen cooled cw-QCLs. The laser was operated in a quasi-cw mode by applying current in rectangular pulses of 120–235  $\mu$ s duration at about 1 kHz repetition rate. This reduced the duty cycle, but did not adversely affect the frequency resolution. A frequency scan of about 2  $\text{cm}^{-1}$  was demonstrated. This strategy was primarily aimed to eliminate fast boiling of the LN2 in the laser Dewar that caused unwanted temperature drift effects seriously restricting the data acquisition time.

In this paper we propose a similar laser driving concept, which we call intermittent scanning, with the aim of reducing the heat dissipation of room-temperature cw-QCLs such that these can be mounted into a TO-3 package. Reducing the power consumption of the laser by one order of magnitude is of prime importance, because it is directly linked to less demanding cooling, temperature control and current sources. Furthermore, we describe a custom developed laser driver based on the intermittent scanning method. This driver eliminates the need for any external electronics for current modulation or costly, ultra-low noise power supplies. Moreover, it allows for an easy control of the duty cycle, current pulses ranging from rectangular shape to pulses featuring different ramp profiles, and pulse duration. Finally, we present methane ab-

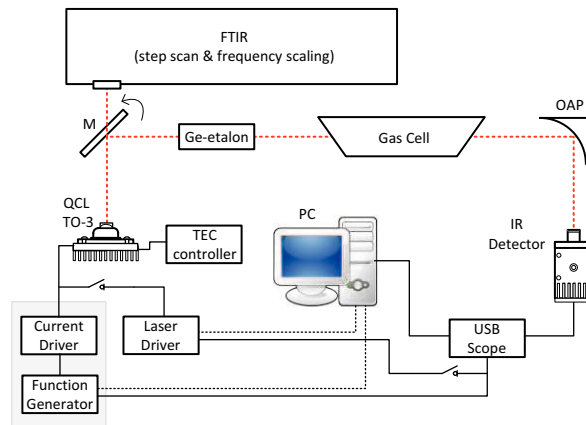


Fig. 2. Schematics of the experimental setup (more details in text).

sorption measurements using the intermittent scanning concept in combination with the custom developed driver to demonstrate its suitability for trace gas spectroscopy.

## 2. Intermittent scanning mode

The most frequently used cw-QCL driving and tuning scheme is the current modulation above threshold at a few kHz. The modulation is usually small and corresponds to less than 10% of the total driving current as schematically shown by Fig. 1(a). However, there is no fundamental reason to continuously apply a DC current to the laser. In principle, the QCL can be turned completely off before the next spectral scan. This is illustrated in Fig. 1(b). The resulting lower duty cycle also means a reduction of average current flowing through the device, so that eventually the heat load remains within the specification of a TO-3. In practice, however, a few questions arise: i) how good is the reproducibility of the heating during a strongly modulated current pulse ii) can we still have a control on the laser tuning characteristics, and iii) would this cycling operation reduce the life-time of the device?

Thermal chirp is the dominating effect which determines the laser current tuning within a current pulse on short time scale ([16, and references therein]). A comparably large current, combined with a small active region volume, leads to high density of power dissipation (tens of kW/cm<sup>2</sup>) and to very intense heating within the active region. In steady state, the active region and the grating temperature is significantly higher than that of the heat-sink. For a typical device the temperature difference between the active region and the heat-sink is typically 30 to 60 °C. This has far reaching consequences for the intermittent scanning operation, since the temperature of the active region is modulated between the heat-sink temperature  $T_0$  and the temperature  $T_{max}(I)$  achieved in steady state with current  $I$  applied to the QCL. Therefore, the intermittent scanning operation also extends the continuous frequency tuning range of the QCL compared to usual current modulation above threshold. This effect is basically the same as the thermal chirp observed in intra-pulse spectroscopy using pulsed QCLs, but on the longer time scale permitted by cw-QCL.

First, to address the concerns about the repeatability and tuning characteristics of the QCL in intermittent scanning mode, we perform time-resolved spectral measurements of the laser chirp using a research grade FTIR (Vertex 80, Bruker) in step scan mode. The experimental setup is schematically shown by Fig. 2. The main elements of the experimental setup consist

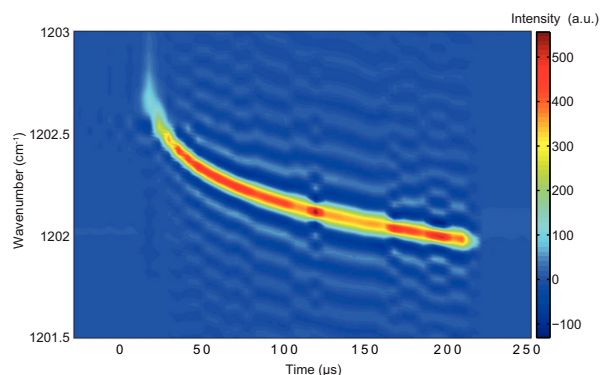


Fig. 3. Time-resolved step-scan measurements of a QCL operated in intermittent scanning mode in a TO-3 package with square pulse modulation. Recorded with  $0.1 \text{ cm}^{-1}$  spectral and  $6 \text{ }\mu\text{s}$  temporal resolution. The periodical ripples around the pulse trace are FT artifacts due to the box-car function, which was selected to obtain the highest resolution.

of a QC laser mounted on a three axis kinematic stage, a frequency analyzer (etalon or FTIR), signal detection and acquisition. A flat mirror (M), mounted on a magnetic kinematic base, can be swapped so that the collimated beam can be coupled either to the FTIR spectrometer or directed across the Ge-etalon. In the preliminary (proof-of-principle) phase, the laser was driven by a low noise current source (QCL1000, Wavelength Electronics). The external current modulation was achieved by a function generator (ArbStudio 1102, LeCroy). This configuration was later replaced by the custom developed laser driver. In both cases the detector signal was recorded with a sampling rate of up to  $125 \text{ MS/s}$  by an USB scope (PicoScope-4227, Pico Technologies).

In the case of step scan by FTIR, the measurement needs to be repeated at every step and the signal time evolution is recorded in slices. However, the measurement time is rapidly increasing with required resolution, which is given by the scanning length. Up to 30 min are required to record high-resolution spectra with  $\Delta f = 0.08 \text{ cm}^{-1}$  without apodization. Figure 3 shows a time-resolved measurement of a QCL emitting at  $8.3 \text{ }\mu\text{m}$  wavelength mounted in a TO-3 package running in intermittent scanning mode. The pulse width is  $200 \text{ }\mu\text{s}$ , the repetition is  $1 \text{ kHz}$ , which corresponds to a duty cycle of 20%. This was sufficient to reduce the average heat dissipation and provide a reliable operation. As expected, there is a rapid frequency tuning at the onset of the pulse in the first  $20 \text{ }\mu\text{s}$ , whereas in the last  $150 \text{ }\mu\text{s}$  it is considerably slower. The measurement indicates low pulse to pulse variations, because otherwise a jitter in the emission frequency would result, due to the averaged intensity at each mirror position in the step scan, in a broadening of the emission line width of the QCL.

For further characterization of the transient tuning behavior, an alternative setup with better temporal and frequency resolution was installed, based on a solid germanium etalon. In this case, the laser beam is directed through the Ge-etalon and then focused, using an off-axis parabolic mirror (OAP), onto a thermoelectrically cooled photovoltaic MCT detector (PVI-4TE-10.6, Vigo Systems). The detector signal is coupled to a high speed (3 dB cut-off frequency  $500 \text{ MHz}$ ) transimpedance preamplifier (VPAC-1000F, Vigo Systems). The detector records the modulated laser amplitude (etalon-fringes) during the laser down-chirp. The spacing of the fringes is given by the free spectral range of the etalon, which is defined as  $FSR = 1/(2n(\lambda, T)L)$ , where  $n(\lambda, T)$  is the refractive index, estimated using the parametrization from [17], and  $L (= 2'')$  is the length of the Ge-etalon. The main advantage of this measure-

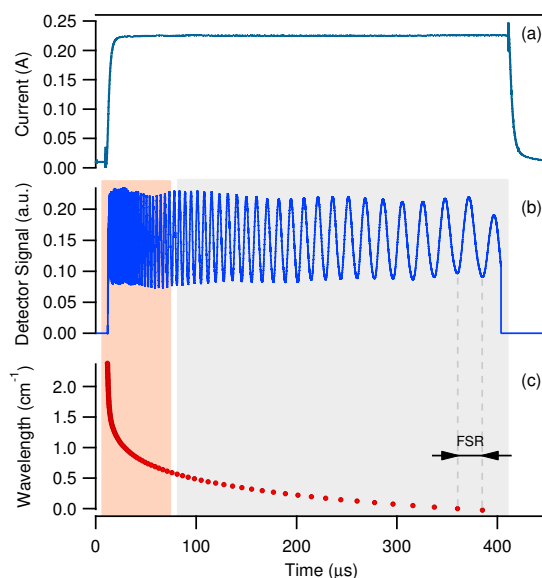


Fig. 4. Frequency chirp measurement of a cw QCL during intermittent scanning with a square current pulse. The current pulse (a) injected to the laser leads to a shift in the laser emission frequency that is revealed by the interference fringes of the Ge-etalon (b). The overall frequency tuning ( $2.5 \text{ cm}^{-1}$  in this case) is then calculated based on the free spectral range ( $FSR \approx 0.02455 \text{ cm}^{-1}$ ) of the Ge-etalon (c).

ment is the speed and the frequency resolution, i.e., a single scan measured with a fast detector allows us to reconstruct the complete frequency chirp. This requires, however, that the source emission is narrow band and single mode, which is verified by the FTIR measurements. In addition, the etalon measurements are inherently relative in frequency. Nevertheless, the combination of both techniques in one setup, as shown in Fig. 2, allows us to make very fast chirp measurements using the etalon, while the absolute frequency is determined with the FTIR in rapid scan mode. Since the translation of the mirror in rapid scan mode is not synchronized with the laser modulation, we require that the modulation frequency is much higher than the duration of a scan. This is easily fulfilled with the modulation frequencies above 1 kHz and scanning frequency of 10 Hz and longer.

The laser thermal chirp measurement for a representative device is shown in Fig. 4. A current pulse generated by the laser driver is presented in the top panel, with the optical response shown in the middle graph. From this optical response it is possible to reconstruct the frequency tuning caused by the chirp as function of time by counting individual fringes. The thermal chirp causes very fast frequency tuning at the beginning of the pulse. This tuning becomes slower as the laser temperature gets closer to the temperature  $T_{max}$  that corresponds to the temperature of the active region at constant current  $I$ . The actual settling time depends on many factors, besides others on laser geometry and on pulse shape. Moreover, it is this property, which determines the length of pulses best suited for spectroscopy. Short pulses lead to very fast tuning representing a challenge for data recording, while long pulses result in a lower repetition rate, less averaged samples and thus, to decreased signal-to-noise ratio. A typical MIR laser requires between 40–80  $\mu\text{s}$  for the heating rate/chirp to slow down sufficiently to be easily recorded with standard, cost-efficient data acquisition boards having 2 to 5 MS/s acquisition rate. For such devices, the strong nonlinearity at the beginning of the chirp as function of the scanning time is undesirable.

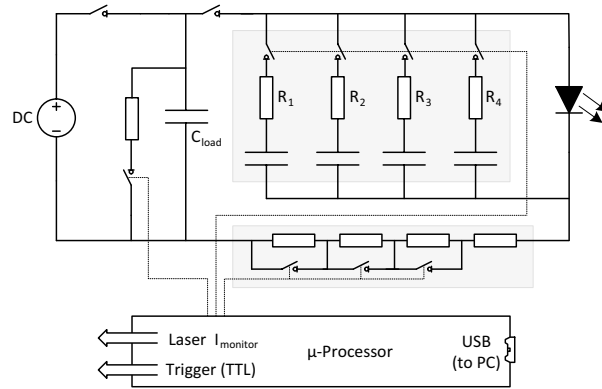


Fig. 5. Schematics of the analog driver developed for intermittent scanning of cw-QCLs. The main parts are: i) loading capacitance ( $C_{\text{load}}$ ) which can be decoupled from the external power supply during pulse generation, ii) alternative pathways for laser current realized by  $RC$ -elements defining the shape of the current pulse that is injected to the laser, iii) additional resistor in series with the laser giving the possibility to change the voltage drop across the laser and also to fine tune the ramp profile, and iv) a microprocessor unit, which allows digital communication with a computer via USB-port. Additionally, the driver delivers a trigger signal (TTL) and offers a laser current monitoring port.

Our investigations of frequency chirp behavior under various driving conditions revealed that the influence of the ramp, superimposed on the top of a square current pulse, is negligible during the period of fast tuning (approx. 20  $\mu\text{s}$ ). After this short period, however, the added ramp led to an almost linear tuning through the rest of the pulse, similar to the standard cw-ramping scheme, with the obvious advantage of a larger tuning range. Thus, applying a ramp on the intermittent scanning seemed to be a promising solution to achieve reliable and spectroscopically useful operation regime for cw-QCLs in TO-3.

### 3. Analog driver for intermittent scanning operation

#### 3.1. Concept and Design

The intermittent scanning mode creates additional options in the design of a laser driver. Given that the laser is off for most of the time ( $\sim 90\%$ ) and the pulses applied to the QCL are relatively long (tens to hundreds of  $\mu\text{s}$ ), it becomes possible to decouple the driver from the power supply during the duration of the pulse using simple passive electronic elements. This represents a clear advantage, because it significantly weakens the demands on the quality (noise and stability) of the power supply. Furthermore, we have opted for a series of capacitors and resistances that define the current ramp. Most laser drivers require a fast and high resolution control signal, usually generated by a digital-to-analog converter (DAC), which is often costly, prone to create ground loop issues, and will always be limited with respect to digital resolution. Alternatively, we propose a series of  $RC$  elements that can be combined to create smooth, analog current ramps of a large variety of shapes.

Figure 5 shows the schematics of the driver electronics, while a detailed description will be covered by another paper. Here we briefly present the operation principle of the driver. The basic idea is to charge a large capacitor (10 mF) through an external power supply during the time when the laser is off. This external power supply is then disconnected through a MOSFET-switch when the laser is turned on. Thus, the QCL is solely driven by the energy stored on the



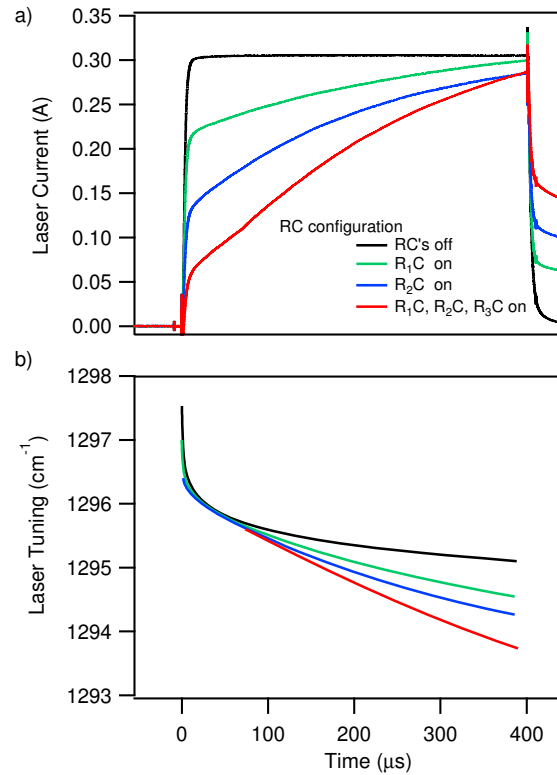


Fig. 6. a) Current ramp profiles measured for different  $RC$ -elements activated and b) the corresponding tuning behavior of the QCL in TO-3 package driven with the custom developed analog driver. We found the same pattern for all the seven QCLs (covering the 4.5, 6 and 8  $\mu\text{m}$  range) tested in this work.

capacitor, which assures a floating output and thereby reducing potential problems related to grounding loops. This approach offers very low noise performance, even when powered by low quality power supplies.

Apart from selecting different voltages on the external power supply, the driver has three built-in load (shunt) resistors  $R_i$ , which can individually be switched into series with the QCL for controlling the current that flows through it. As previously mentioned, one key factor for the intermittent operation is the generation of a ramp on top of the current pulse to control the tuning rate. This is achieved through four individual  $RC$  elements, connected in parallel to the QCL, which can be independently switched in any combination, leading to 16 ( $2^4$ ) possible configurations. The capacitance of each  $RC$  element is 14  $\mu\text{F}$ . To generate pulse shapes with varying time-constants, the resistors of the individual  $RC$  elements are different ( $R_1 = 22 \Omega$ ,  $R_2 = 12 \Omega$ ,  $R_3 = 7.5 \Omega$ ,  $R_4 = 4 \Omega$ ). All switches,  $RC$  elements and load-resistors are controlled through a microcontroller connected via USB to a PC. The same microcontroller is used to generate a trigger signal (TTL) synchronized with the laser pulses. Using this driver, it is therefore possible to generate a wide variety of pulses with the same analog electronics.

The output impedance of the device is mainly determined by the resistors in series with the laser and the active  $RC$  elements. Therefore, depending on the selected configuration, it may vary between 0.6 and 8  $\Omega$ . Also the power consumption of the driver strongly depends on the operating condition. Simulation (LTspice, Linear Technology) of a typical configuration, i.e., a

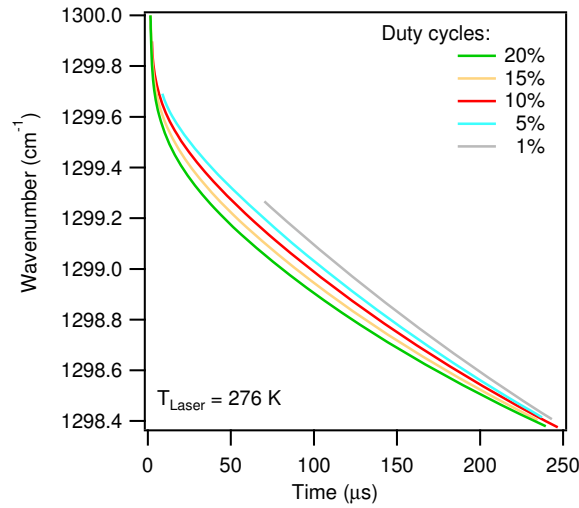


Fig. 7. Tuning behavior as a function of duty cycle at constant pulse length.

pulse length of 400  $\mu\text{s}$ , 10% duty cycle, 9.2 V supply voltage,  $R_2C$  switched on, and an equivalent shunt resistor of 4  $\Omega$ , resulted in average dissipated power of 0.3 W. This corresponds to 14% of the dissipated power in an equivalent cw operation regime. The average power of the driving circuit was in this case 0.4 W. The additional glue logic (mainly microprocessor), which is not optimized for low power, consumes another 0.9 W. Compared to typical cw-QCL driving setups involving DC power supply, laser driver, function generator, and laser heat-sink temperature controller, the overall power consumption of our driver is easily lower by one or two orders of magnitude.

### 3.2. Driver Characterization

A simple absorption experiment allows us to quantify the frequency stability of a laser operated in intermittent regime and assess the suitability of the intermittent scanning approach for spectroscopic measurements. Therefore, we extended our experimental setup (Fig. 2) with a single pass absorption cell, 14 cm long, filled with 1% methane in nitrogen at 80 hPa. The light source is a DFB QCL, mounted in a TO-3 housing with collimating optics, emitting around 1295  $\text{cm}^{-1}$ . This spectral region covers strong methane absorption lines and it is almost free of water absorption. The laser was driven with our custom developed driver in intermittent regime up to 20% duty cycle, powered by a programmable DC-power supply (HMP4040, HAMEG Instruments). The repetition rates were varied between 250 Hz and 1 kHz.

Our first aim was to characterize the frequency down-chirp as function of different current ramp profiles that can be generated with our custom driver. Figure 6(a) shows a set of different ramp configurations. The square pulse is generated when all  $RC$  elements are turned off, while the two scans with medium rates are generated with one  $RC$  element switched on (either  $R_1C$  or  $R_2C$ ), and the fourth scan is achieved with three different  $RC$  elements switched on ( $R_{1-3}C$ ). The QCL temperature is maintained at 15°C. The pulse is 400  $\mu\text{s}$  long with a duty cycle of 10%. Figure 6(b) shows the corresponding frequency tunings achieved with different current ramps. The maximal frequency range covered within a scan spans  $\sim 2.5 \text{ cm}^{-1}$ . The square pulse leads to pronounced nonlinear behavior at the beginning of the pulse. The pulse shaping with three  $RC$  elements results in a more linear tuning behavior over the entire tuning range at the expense of a slightly reduced tuning range of 1.8  $\text{cm}^{-1}$ . These results demonstrate that

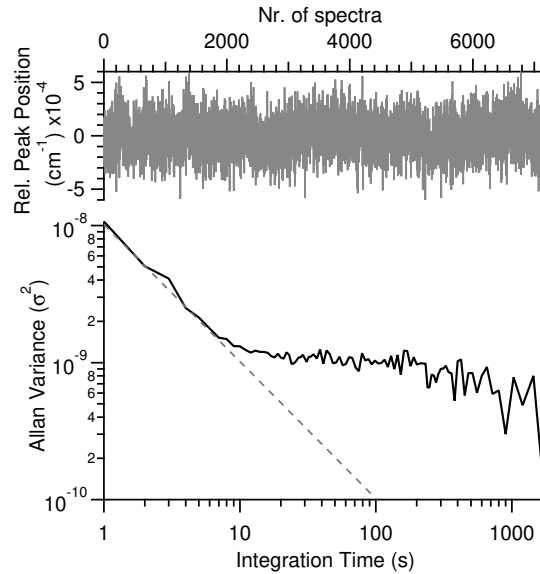


Fig. 8. Determination of the frequency stability of the intermittent scanning with the custom-developed driver. The position of a methane absorption line is recorded over two hours (top) and the corresponding Allan variance plot as a function of integration time is calculated (bottom).

using *RC* elements for pulse shaping is a good solution for generating a wide variety of current ramps, some of which feature large linear tuning ranges. For comparison, the widely used current modulation approach for cw-QCL tuning can achieve up to 1 cm<sup>-1</sup> spectral coverage, but a spectral range of 0.5 cm<sup>-1</sup> is more typical. However, the possibility of a larger tuning, as in the case of intermittent scanning, opens new opportunities for multi-species gas detection applications.

Another evident question is the tuning behavior as a function of duty cycle. The load and unload cycles of the capacitor in the custom made driver might result in strongly varying currents that flow through our device, thus changing the chirp characteristics of the laser. Furthermore, the duty cycle has an effect on the laser temperature and thus on its frequency. Therefore, we investigated the influence of changing duty cycle between 1 and 20% by varying the repetition rate of the current pulse, while keeping the pulse length and shape the same. The results (see Fig. 7) show that there is only a small and very consistent effect of the duty cycle on the laser frequency. This property is very convenient, because the frequency and tuning behavior for any duty cycle can be well anticipated based on any single measurement. Moreover, this property can be used to compensate slight thermal-drifts of the QCL by simply adjusting its duty-cycle. This approach represents a clear advantage over the heat-sink temperature correction method, because it has an immediate, direct and smooth effect. In some particular situations it may even make the laser TEC obsolete.

The long-term stability of the driver was assessed by tracking one of the absorption lines of methane over an extended period of time, assuming that the performance is limited mainly by the driver. Figure 8 shows the time evolution of the measured peak position and the corresponding Allan variance plot [18]. The laser was operated with 100 μs long pulses at 10% duty cycle. A number of 400 individual absorption spectra, recorded at a sampling rate of 62.5 MS/s, were co-added in the oscilloscope's buffer memory and transferred to the PC at a rate of 1 Hz.

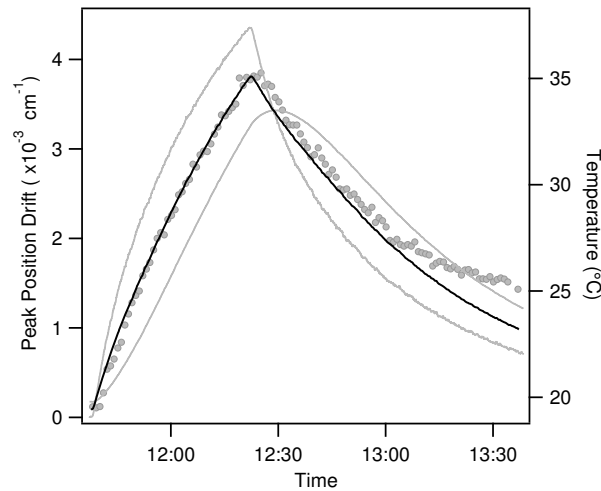


Fig. 9. Influence of varying temperature on the output current of the custom-made driver. The drift in the absorption line position (gray circles) tightly correlates with the average temperature (black line) measured by two thermistors (gray lines) monitoring the driver and the surrounding air temperature, respectively.

The peak position shows a  $\sim 1 \times 10^{-4} \text{ cm}^{-1}$  ( $1\sigma$ ) scan-to-scan variation over the full record, while the Allan-variance has a minimum after 10 s, corresponding to a frequency stability of  $3.2 \times 10^{-5} \text{ cm}^{-1}$ . An even better ( $10\times$ ) stability performance is observed when considering the drifts in the relative frequency difference of two neighboring absorption lines. This indicates that the measurements may be influenced by other factors like the PID-control of the QCL's heat-sink or temporal instabilities of the trigger signal ( $\pm 2 \text{ ns}$  jitter). Nonetheless, the observed frequency stability is comparable with typical laser line widths (850 kHz at 0.3 s observation time) reported for free-running DFB-QCLs based on frequency noise power spectral density (PSD) measurements [19]. Our high-end instruments (see e.g. [22]) using cw operation for similar QCLs in LLH with water cooled heat-sink and ultra-low noise (few  $\text{nA}/\text{Hz}^{1/2}$ ) laser drivers can reach frequency stabilities of  $1.6 \times 10^{-5} \text{ cm}^{-1}$ . This is about a factor two better than what we found for the intermittent scanning, but on the expense of much more elaborated hardware for temperature and injection current stability. For most gas sensing applications a value of  $10^{-4} \text{ cm}^{-1}$  is largely enough, considering the absorption line widths of about  $10^{-2} \text{ cm}^{-1}$  at full width half maximum (FWHM) in the mid-infrared at gas pressures  $< 100 \text{ hPa}$ .

An important factor that usually influences the long-term stability of a spectrometer is the temperature dependence of the driving electronics. To quantify this effect, we placed our custom made driver into an insulated box in which we could cycle the temperature on demand via Peltier elements. Two thermistors were used to monitor the temperature of the driver electronics and the air inside the box, respectively. The box temperature was then cycled from  $18^\circ\text{C}$  to  $38^\circ\text{C}$  and back. The external DC power supply was at constant laboratory temperature. Again, we tracked the peak position of a  $\text{CH}_4$  absorption line. As shown in Fig. 9, the drift in the line position closely correlates with the mean temperature of the two temperature sensors. The derived temperature dependence for our driver is  $2.3 \times 10^{-4} \text{ cm}^{-1}/\text{K}$ . Considering the typical laser dynamic response, this would translate into a temperature coefficient of about  $10 \text{ ppm}/\text{K}$  that is comparable to the values found for commercial laser drivers.

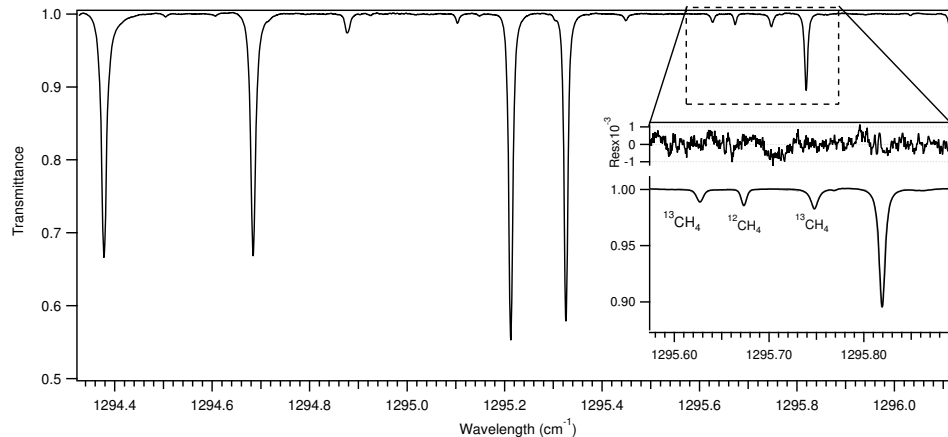


Fig. 10. Measured transmission spectrum of 1% methane at 80 hPa in a single pass 14 cm long gas cell measured in intermittent scanning mode with a spectral resolution of  $3.4 \times 10^{-4} \text{ cm}^{-1}$ . The laser is operated in a TO-3 package and is driven by the custom made driver. The inset graph shows a close-up view of a spectral range with isotopologues of  $\text{CH}_4$  fitted to Voigt profiles with the associated fit-residuals.

### 3.3. Spectroscopic application

Finally, to assess the suitability of the driver and the intermittent scanning concept for high resolution laser absorption spectroscopy, we measured methane (1%) with a spectral coverage of about  $1.8 \text{ cm}^{-1}$  around  $1295 \text{ cm}^{-1}$ . The absorption spectrum (Fig. 10), containing 8192 data points, was recorded at a sampling rate of 15 MS/s and averaged over 2000 scans in the buffer memory of the oscilloscope. Using a  $350 \mu\text{s}$  long ramp at 10% duty cycle, it resulted in an effective spectral data acquisition rate of 0.1 Hz. This corresponds to the optimal averaging time obtained from the Allan variance analysis (Fig. 8). The relative frequency scale was determined using the etalon fringes as described in Sect. 2, and calibrated from the known frequencies of the observed transitions by using the HITRAN database [20]. The absorption lines in a narrow spectral range were then fitted to a Voigt-profile [21], as shown by the inset in Fig. 10. The selected spectral window contains absorption lines of both the main isotopologue  $^{12}\text{CH}_4$  and the  $^{13}\text{CH}_4$  species. Therefore, we could also assess the possibility of measuring the corresponding isotope ratio. Running the measurements continuously over 15 hours, we obtained a standard deviation ( $1\sigma$ ) of the  $^{13}\text{CH}_4/^{12}\text{CH}_4$  ratio of 4 ‰ over the whole period. Ratioing the absorption peaks removed correlated noise terms and allowed for extended averaging. At the optimal integration time of 280 s the measurement precision was 0.45 ‰. Scaled to state-of-the-art spectroscopic setups with over 200 m optical path length (see e.g. [23]), this would correspond to a precision of about 1.5 ‰ for  $^{13}\text{CH}_4/^{12}\text{CH}_4$  at atmospheric abundance. Thus, the present performance of our setup is lower by about one order of magnitude, but we should note that the measurements were done without any temperature stabilization of the optical setup (decisive for isotope ratio measurements), nor background subtraction or fringe suppression, and at 10% duty cycle only. Given the relatively low frequency scanning, the spectroscopic system is mainly dominated by the  $1/f$  noise, thus the penalty due to the reduced duty cycle scales by  $\sqrt{n}$ , where  $n$  is the number of acquired spectra for a given acquisition time. As further optimizations of the spectroscopic setup are readily possible, we conclude that the proposed intermittent scanning approach and the described laser driver are highly promising with respect to performance, compactness and cost efficiency.

#### 4. Conclusion

In this paper we demonstrate the successful operation of a cw-QCL in a TO-3 packaging with collimating optics implementing the intermittent modulation concept. This operation scheme effectively reduces the power consumption and correspondingly the average heat dissipation of a cw-QCL below 1 W by completely shutting down the driving current after each spectral scan for long enough time for the laser to cool down. Laboratory investigations of decisive parameters, involving repeatability and tuning characteristics, revealed stable operation behavior that allows the application of the intermittent scanning approach in molecular absorption spectroscopy. To fully explore the advantage offered by this concept, we developed a cost effective, compact, largely analog, yet flexible laser driver with low power consumption ( $< 1$  W) operating without any external current modulation or high compliance power supplies. Further built-in flexibilities are the possibility of varying duty cycle and defining current pulses ranging from rectangular shape to pulses featuring different ramp profiles. The driver assures low-noise operation, thus a high frequency stability ( $3.2 \times 10^{-5} \text{ cm}^{-1}$ ) of the laser, while selecting optimum ramp shape leads to large and nearly linear frequency tuning ( $> 1.5 \text{ cm}^{-1}$ ) of the QCL. These features largely compensate for potential loss in signal-to-noise ratio due to the reduced duty-cycle and open the way towards the development of compact, cost and power efficient gas sensors based on QCLs. The driver was continuously operated for a period of two months without any indication for degradation in the laser characteristics. The suitability for molecular spectroscopy was assessed by analyzing methane absorption lines in the  $7.7 \text{ }\mu\text{m}$  spectral region.

#### Acknowledgments

This work was funded by the Commission for Technology and Innovation (CTI) under grant number 13453.1 PFFLI-NM and NanoTera (<http://www.nano.tera.ch>).